SINERGI Vol. 29, No. 2, June 2025: 555-562
http://publikasi.mercubuana.ac.id/index.php/sinergi
http://doi.org/10.22441/sinergi.2025.2.025

Instrumented model slope to investigate the influence of rainfall and slope gradient on matric suction

Jestin Jelani[1]*, Aina Syahirah Ahmad Ishak[1], Nordila Ahmad[1], Zuliziana Suif[1], Wan Mohamad Adham Hanis Wan Suhaili[1], Ahmad Loqman Ahmad Mazuki[2], Latifah Sarah Supian[2]
[1]Civil Engineering Department, Engineering Faculty, National Defence University of Malaysia, Malaysia
[2]Electrical and Electronics Engineering Department, Engineering Faculty, National Defence University of Malaysia, Malaysia

Abstract
Prior researchers indicated that prolonged and heavy rainfalls primarily trigger major landslides in Malaysia. This study was carried out to investigate the influence of rainfall on the matric suction of silty sand slopes through a small-scale model. A 35° and 45° slope (namely EXP1 and EXP2) models were built using soil samples from the former landslide site at Kemensah Heights, Selangor, Malaysia. Two types of sensors were used to measure matric suction and rainfall intensities using Watermarks 200SS Soil Moisture Sensor and Hydreon rain gauge RG-15, respectively. The elapsed time since the beginning of the rainfall was recorded using two cameras placed at the front and side of the slope model to observe progressive failure. The results showed that the initial matric suction with a value of 250 kPa is significantly reduced and approached 0 kPa when the range of cumulative rainfall intensity is between 30 and 36.75 mm/min and 5.25 and 6.75 mm/min recorded by PP1 and PP2 in EXP1 and EXP2, respectively. The results indicate that the reduction in matric suction induced by rainwater infiltration is the triggering mechanism of slope failure. It has also been noticed that rainfall infiltration increases with decreasing slope gradients. However, a small gradient slope requires longer rainfall prior to failure. A slope with a high gradient has a longer time before failure occurs after loss of matric suction than a low slope gradient.

Keywords:
Matric Suction;
Rain Gauge;
Rainfall-induced Landslide;
Slope Gradient;
Watermarks;

Article History:
Received: November 22, 2024
Received: December 20, 2024
Accepted: January 28 2025
Published: May 17, 2025

Corresponding Author:
Jestin Jelani
Civil Engineering Department, Engineering Faculty, National Defence University of Malaysia, Malaysia
Email: jestin@upnm.edu.my

INTRODUCTION

Landslides are significant geological risks that take place in mountainous or hilly terrain, causing severe damage to property and the loss of lives. Landslides are described as the movement of rocks, debris, or soil induced by gravity involving quick or slow movement close to the slope surface. Several factors influence landslides, among which can be classified into two factors: internal and external. The external factors triggered by earthquakes, volcanic activities, human interference, slope steepness, surcharge load, and rainfall, to name a few [1, 2, 3]. The internal factors are due to changes in intrinsic soil stress caused by pore pressure, matric suction, and shear strength properties (i.e., internal friction angle and cohesion) [4][5].

Massive landslides in Malaysia are mainly attributed to frequent and prolonged rainfalls [6,7,8]. Methods based on the measurement of rainfall effect on slope instability (later known as rainfall-induced landslide) have been developed for landslide prediction in the previous studies either through rainfall threshold value [9][10] or sensor-based monitoring [11, 12, 13]. The explanations of landslides that occur after rainfall have been elucidated in literature, where rainwater infiltration causes a decrease in soil matric suction and shear strength, eventually resulting in slope failure. The failure mechanism occurs when precipitation permeates the slope and completely saturates the soil. Consequently, the moisture content of the soil is elevated, leading to a subsequent decrease in matric suction and shear strength. The decrease in soil shear strength leads to the instability and eventual failure of the slope [14][15]. Upon full saturation of the soil slope, the soil suction ceases entirely, and positive pore water pressure forms on the slope [16]. After or during intense rainfalls, after extended periods of rain, or with a significant delay to downpour events, one can notice the mass movements, debris, and mud flows.

Several field and laboratory experiments have been conducted to investigate the effects of rainfall on slope stability in different types of soil. The significance of hydrological and geotechnical factors of a slope on rainfall-induced landslide was investigated by [17] through a series of parametric investigations. The study indicates that several factors, including rainfall intensity, soil characteristics, groundwater table, and slope dimensions, substantially impact the instability of a slope caused by rainfall. In conclusion, the study found that the higher slope angle causes a lower safety factor. Another research by [9] presented suction distribution in the soil during critical rainfall patterns to determine the safety factor of different types of soil. Recent research by [18][19] presented the results of a slope model subjected to artificial rainfall. It is instrumented with a pore pressure sensor to develop a time prediction method for landslides and elucidate the reduction shear strength of soil, respectively.

Very limited studies have been found in the literature combining rainfall intensity, matric suction, and slope gradient to determine slope instability. In this study, combinations of the parameters were used to investigate the influence of rainfall on matric suction for the small-scale instrumented model slope made of silty sand soil subjected to artificial rainfall.

METHOD

Soil Sample Collection

The disturbed and undisturbed soil samples were collected at the former landslide site at Kemensah Heights, Selangor, Malaysia, which occurred on 18 September 2021. The landslide translated approximately 2536 m^2 of earth, blocking a river downstream of the slope, as shown in Figure 1. Based on local news, the landslide occurred after three days of rainfall. The collected samples were stored in a sealed plastic bag and then air-dried for a few weeks (Figure 2).

Figure 1. Landslide incident at Kemensah Heights on 18 September 2021


Figure 2. Soil samples were air-dried.

The residual soil of the study area is mainly from weathered granitic rock.

Laboratory Test

A series of laboratory tests were conducted to determine the soil properties, as summarised in Table 1. The tests include sieve analysis, Atterberg Limit, particle density, permeability, shear strength, and compaction.

Experimental Test

The dimensions of the acrylic box used in this study are 152 cm in length, 102 cm in height, and 51 cm in width, as shown in Figure 3 [2]. A modified PVC pipe of 15 mm diameter with an attachment of eight water sprinklers was installed above the slope to provide artificial rainfall, as shown in Figure 4.

Table 1. Laboratory test and standard of testing.

No	Test	Standard of Testing
1	Sieve Analysis	BS1377:1990, Part 2
2	Atterberg Limit	BS 1377:1990, Part 2
3	Particle Density	BS 1377:1990, Part 2
4	Permeability	BS 1377:1990, Part 5
5	Direct Shear	BS1377:1990, Part 7
6	Compaction	BS 1377:1990, Part 4

The box was set up at a 6° angle, approximately 16 cm elevated from the floor, to prevent water puddling at the toe of the slope. A channel was built at the front to allow excess water to drain out to a nearby drainage.

A 35° and 45° slope models were built inside the box and compacted for every 5 cm lift with 30 blows using a modified square hand compactor. The proposed slope angles are selected based on previous study [8]. The average bulk density, p_b, of compacted soil was calculated using (1). The relative compaction of soil inside the box was compared to a laboratory compaction test to determine its relative density, R, expressed in (2).

$$pb = \frac{Weight\ of\ soil\ in\ box\ (kg)}{Volume\ of\ box (m^3)}, \qquad (1)$$

$$Relative\ compaction : R\ (\%) = \frac{\lambda\ d(field)}{\lambda\ d\ max\ (lab)}. \qquad (2)$$

This study adopted a rainfall intensity of 45 mm/hr to represent the medium rainfall categories in Malaysia based on the average rainfall intensity defined by Urban Stormwater Management Malaysia. The rainfall intensity was measured using Hydreon rain gauge RG-15, with nominal accuracy of within ±10%, capable of operating within temperatures of -40°C to +60°C. The matric suction was determined using a soil moisture sensor (Watermarks 200SS by Irrometer) to monitor the changes in suction during rainfall infiltration. The Watermarks sensor can measure matric suction ranges between 0 kPa to 200 kPa. Before its installation, the calibrated sensors were soaked in the water for one or two days to allow air removal from the sensor. Then, wet silica sand was used to wrap the sensor with an approximate thickness of 3 cm, as shown in Figure 5a. Subsequently, the sensors were wrapped with a perforated thin fabric to contain the sand and allow water to seep in or out (refer to Figure 5b). The wrap is tied, and the wrapped sensors are again soaked in water for one or two days before installation, as shown in Figure 5c.

The suction values were set to continuously and automatically register the data every minute. The readings of both types of sensors were monitored using Campbell Scientific Data Logger CR350, equipped with 16 channels.

During the construction of the slope model, two Watermarks 200SS soil moisture sensors (PP1 and PP2) were installed at a depth of 5 cm. The schematic representation of the slope model and arrangement of sensors are presented in Figure 6. Two cameras were positioned at the front and side of the box to capture progressive slope failure. Table 2 summarises the experimental program of this study.

Figure 3. Dimension of acrylic box

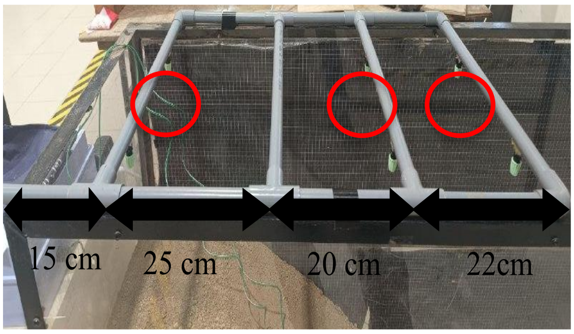

Figure 4. Position of eight water sprinklers attached to modified PVC pipes placed on the top of the slope model

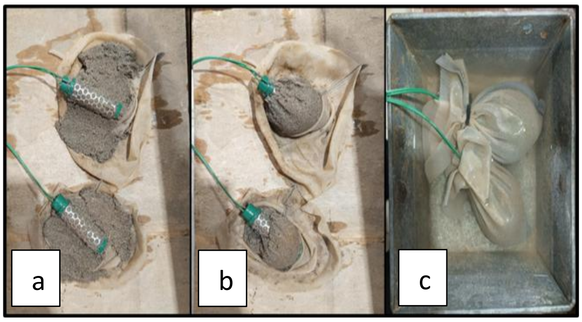

Figure 5. Preparation of Watermarks 200SS sensors: (a) wet silica sand is used to wrap the sensors, (b) thin fabrics were used to contain the silica sand and sensors, and (c) soaked the prepared sensors in water for one or two days before testing

Table 2. Experimental program

No. of Exp	Slope Angle (°)	Rainfall Intensity (mm/hr)	Duration of rainfall (min)
EXP1	35	45	60
EXP2	45	45	60

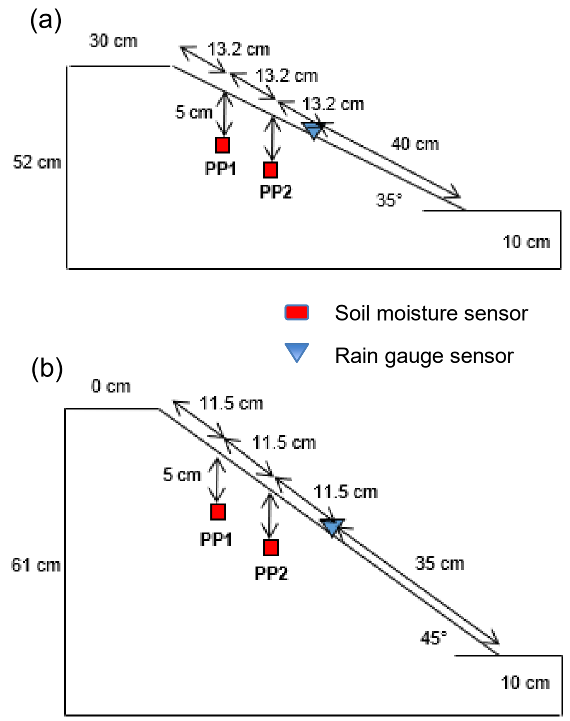

Figure 6. Schematic representation of slope model and position of sensors for slope angle (a) 35° and (b) 45°

RESULTS AND DISCUSSION

Laboratory Test Results

The result of the sieve analysis is shown in Figure 7, which comprises 16% clay, 28% silt, 42% sand, and 14% gravel. Based on the British Soil Classification System, the soil is classified as Silty Sand. The result of the compaction test is shown in Figure 8. The relative compaction, *R*, of the soil in the box, is approximately 70%. Table 3 summarises the results of laboratory testing.

Observation of silty sand slope subjected to 45 mm/hr rainfall intensity

The signs of failure in all experiments were observed at 20-, 40-, and 60-minute intervals. Based on the results, the types of failure for EXP1 and EXP2 are similar, which is categorised as gully erosion.

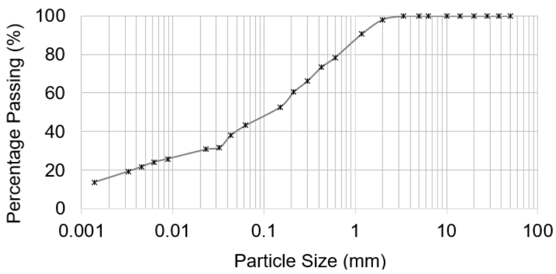

Figure 7. Particle size distribution of soil

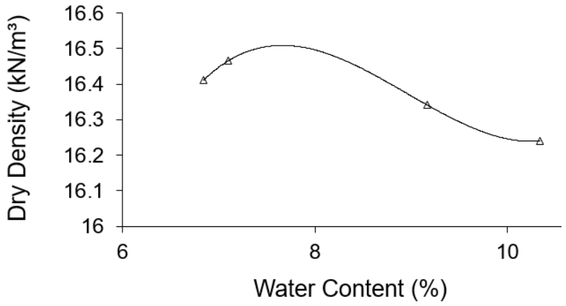

Figure 8. Soil compaction test results

Table 3. Summary of laboratory test results

Properties	Results
Liquid Limit (%)	40
Plastic Limit (%)	26
Plastic Index (%)	14
Particle density (Mg/m^3)	2.63
Permeability (10^{-3} mm/s)	5.96
Max dry unit weight (kN/m^3)	16.51
Optimum moisture content (%)	7.3
Cohesion (kPa)	5
Friction angle (°)	41

They occur when the soil at a shallow depth reaches full saturation. The runoff water begins to flow down the slope surface and subsequently erodes the surface [20].

Gully deformation and duration of slope failure are more likely influenced by slope gradient. The average gully deformation in EXP1 and EXP2 are 9 cm and 17 cm, respectively. The findings indicate that the higher the slope gradient, the higher the slope erosion, which is congruent with findings by [21]. The duration of slope failure for EXP2 occurred 50% faster than EXP1. The results imply that as the slope gradient increases, the duration of failure and gullies dimension increase under similar rainfall intensities. Table 4 illustrates the differences in slope conditions for EXP1 and EXP2 from the front view.

Table 5 compares the side view of the slope before and after the experimental test. For EXP1, the depth of rainwater infiltration is more compelling than EXP2 due to the slow movement of surface runoff, which gives it time to infiltrate the soil. However, the failed time for EXP1 is 50% longer than that of EXP2. The results imply that infiltration increases with decreasing slope gradient. However, a smaller gradient slope requires longer rainfall before failure [22].

Table 4. An elapsed time since the onset rainfall for EXP1 and EXP2 from the front view.

No Experiment	Slope angle (°)	Before	20 minutes	40 minutes	60 minutes
EXP1	35				
EXP2	45				

Table 5. Comparison of slope conditions, failure duration, and gullies formation for EXP1 and EXP2 subjected to rainfall intensity of 45 mm/hr.

No. Exp	EXP1	EXP2
Before		
After		
Durations of slope failure	Required 40 minutes to failed	Required 20 minutes to failed
Gullies Deformation	Average vertical deformation from laboratory test is 9 cm	Average vertical deformation from laboratory test is 17 cm

Relationship of cumulative rainfall intensity, rainfall duration, and matric suction

Figure 9 shows the graph of cumulative rainfall intensity, matric suction, and rainfall duration for both experiments. The maximum matric suction values for both experiments are approximately 250 kPa. As the rainfall progresses, the value suddenly drops to 0 kPa once the infiltrated rainfall reaches the sensor at cumulative rainfall between 30 to 36.75 mm/min and 5.25 to 6.75 mm/min recorded by PP1 and PP2, respectively.

The difference in soil suction distribution patterns is due to the variability of slope angle and position of sensors [23][24]. Failure states, indicated by the red line for EXP2, are approximately 11 to 13 minutes delayed by the sudden drop of matric suction. Whereas for EXP1, it occurs faster in less than 2 minutes due to the influence of slope gradient. A slope with a high gradient has a longer time before failure takes place after loss of matric suction compared to a low slope gradient. The study's findings conclude that the loss of matrix suction indicates a slope failure, showing that matric suction decreases as water infiltrates into the slope [25].

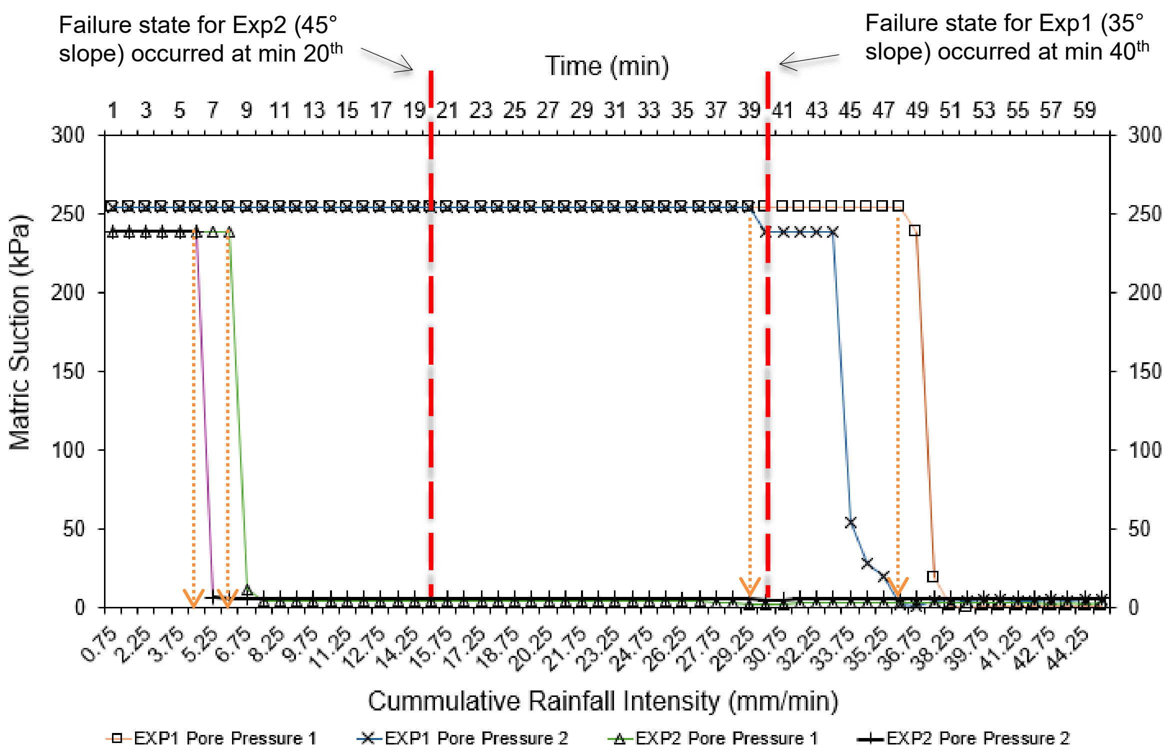

Figure 9. Graph the relationship between cumulative rainfall intensity with matric suction for EXP1 and EXP2 subjected to artificial rainfall.

CONCLUSION

There are a few conclusions drawn from the study as follows:

- The initial matric suction value of 250 kPa is significantly reduced. It reaches nearly 0 kPa once the infiltrated rainfall reaches the sensor when the range of accumulative rainfall intensity is between 30 to 36.75 mm/min and 5.25 to 6.75 mm/min recorded by PP1 and PP2.
- A slope with a high gradient has a longer time before failure takes place after loss of matric suction compared to a low slope gradient.
- For EXP2, the failure occurred 50% faster than that of EXP1. The average gullies' deformation in EXP1 and EXP2 are 9 cm and 17 cm, respectively. The findings indicate that slope angle has an influence on the duration of failure and gullies' dimension under similar rainfall intensities.

ACKNOWLEDGMENT

The authors wish to thank the National Defence University of Malaysia for funding and supporting this project under the grant, with project code: UPNM/2023/GPJP/TK/2

REFERENCES

[1] C. Gallage, T. Abeykoon, and T. Uchimura, "Instrumented model slopes to investigate the effects of slope inclination on rainfall-induced landslides," *Soils and Foundations*, vol. 61, no. 1, pp. 160–174, 2021, doi: 10.1016/j.sandf.2020.11.006.

[2] A. S. Ahmad Ishak, J. Jelani, S. Y. Wong, Z. Suif, and A. L. A. Mazuki, "Experimental and Numerical Study on the Behaviour of Silica Sand Slope Model," *J Teknol*, vol. 86:1, no. 2024, pp. 165–173, 2024.

[3] A. S. Ahmad Ishak, J. Jelani, S. Y. Wong, Z. Suif, and A. L. Ahmad Mazuki, "Stability Analysis of a Silica Sand Slope Model Subjected To Surcharge Load Using LEM and FEM Methods," *International Journal of GEOMATE*, vol. 27, no. 121, pp. 128–135, Sep. 2024, doi: 10.21660/2024.121.g13442.

[4] D. Meng et al., "An insight into the association between volatile and other active components of sea buckthorn berries in barren soils of western China," *Food and Humanity*, vol. 2, 2024, doi: 10.1016/j.foohum.2024.100293

[5] X. Wang, K. C. Wang, T. Deng, F. Wang, Y. F. Zhao, J. Li, Z. Huang, J. W. Wang & W. H. Duan, " Contribution of soil matric suction on

slope stability under different vegetation types," *Journal of Soils and Sediments*, vol. 24, pp .575–588, 2024, doi: 10.1007/s11368-023-03653-1

[6] A. M. Taib, M. F. Law, R. P. Munirwan et al., "The stability of natural and man-made unsaturated slopes influenced by different rainfall patterns," *Environmental Science and Pollution Research*, 2024, doi: 10.1007/s11356-024-34775-9

[7] O'Brien, M.J., Hector, A., Ong, R. et al., "Tree growth and survival are more sensitive to high rainfall than drought in an aseasonal forest in Malaysia," *Communications Earth & Environment*, vol. 5, ID: 179, 2024, doi: 10.1038/s43247-024-01335-5

[8] J. Jelani, M. S. S. Abdul Rahman, S. Sojipto, W. M. S. Wan Mohamed Sabri, L. M. Lee, and N. Ahmad, "Geotechnical Investigation of a Landslide Incident In Hulu Kelang, Malaysia," *International Journal of GEOMATE*, vol. 27, no. 120, pp. 138–145, Aug. 2024, doi: 10.21660/2024.120.g13382.

[9] H. Q. Yang and L. Zhang, "Bayesian back analysis of unsaturated hydraulic parameters for rainfall-induced slope failure: A review," *Earth-Science Reviews*, vol. 251, ID: 104714, April 2024, doi: 10.1016/j.earscirev.2024. 104714

[10] F. Fusco *et al.*, "Physically based estimation of rainfall thresholds triggering shallow landslides in volcanic slopes of Southern Italy," *Water (Switzerland)*, vol. 11, no. 9, Sep. 2019, doi: 10.3390/w11091915.

[11] C. Y. Hong, Y. F. Zhang, M. X. Zhang, L. M. G. Leung, and L. Q. Liu, "Application of FBG sensors for geotechnical health monitoring, a review of sensor design, implementation methods and packaging techniques," *Sens Actuators A Phys*, vol. 244, no. 2016, pp. 184–197, 2016, doi: 10.1016/j.sna.2016.04. 033.

[12] H. Xu, F. Li, W. Zhao, S. Wang, Y. Du, and C. Bian, "A high precision fiber bragg grating inclination sensor for slope monitoring," *J Sens*, vol. 2019, 2019, doi: 10.1155/2019/1354029.

[13] A. S. Ahmad Ishak, J. Jelani, S. M. F. Syed Mohd Dardin, Z. A. Rashid, and Z. Suif, "Concept Development of Inclinometer for Real-Time Data Collection in Slope Movement Detection," *Journal of Engineering Science and Technology*, vol. 18, no. 1, pp. 132–144, 2023.

[14] A. N. C. Ghani, A. M. Taib, and D. Z. A. Hasbollah, "Effect of Rainfall Pattern on Slope Stability," *Lecture Notes in Civil Engineering*, vol. 62, pp. 887–892, 2020, doi: 10.1007/978-981-15-2184-3_115.

[15] N. Gofar, L. M. Lee, and A. Kassim, "Stability of Unsaturated Slopes Subjected To Rainfall Infiltration," *Faculty of Civil Engineering*, pp. 158–167, 2010.

[16] K. Sasahara, "Prediction of the shear deformation of a sandy model slope generated by rainfall based on the monitoring of the shear strain and the pore pressure in the slope," *Eng Geol*, vol. 224, no. October 2016, pp. 75–86, 2017, doi: 10.1016/j.enggeo.2017.05.003.

[17] H. Rahardjo, T. H. Ong, R. B. Rezaur, and E. C. Leong, "Factors Controlling Instability of Homogeneous Soil Slopes under Rainfall," *Journal of Geotechnical and Geoenvironmental Engineering*, vol. 133, no. 12, pp. 1532–1543, Dec. 2007, doi: 10.1061/(asce)1090-0241(2007)133:12(1532).

[18] K. Sasahara, "Time-Prediction Method of the Onset of a Rainfall-Induced Landslide Based on the Monitoring of Shear Strain and Pore Pressure," in *4th World Landslide Forum*, 2017, pp. 93–101. doi: 10.1007/978-3-319-53487-9.

[19] Z. Guo, Q. Huang, Y. Liu, Q. Wang, and Y. Chen, "Model experimental study on the failure mechanisms of a loess-bedrock fill slope induced by rainfall," *Eng Geol*, vol. 313, no. December 2022, 2023, doi: 10.1016/j.enggeo.2022.106979.

[20] X. Xu, F. Zheng, G. V. Wilson, and M. Wu, "Upslope inflow, hillslope gradient and rainfall intensity impacts on ephemeral gully erosion," *Land Degrad Dev*, vol. 28, no. 8, pp. 2623–2635, 2017, doi: 10.1002/ldr.2825.

[21] X. Xu, F. Zheng, and G. V. Wilson, "Flow hydraulics in an ephemeral gully system under different slope gradients, rainfall intensities and inflow conditions," *Catena (Amst)*, vol. 203, no. 26, 2021, doi: 10.1016/j.catena.2021.105359.

[22] N. Gofar, E. N. Pangestika, Y. Harianto, H. Gumay, and A. Satyanaga, "Effect of near-surface heterogeneities on the pore-water pressure distribution and slope stability," *Sinergi*, vol. 28, no. 2, pp. 327-336, 2024, doi: 10.22441/sinergi.2024.2.012

[23] S. N. Hamizak, Z. Suif, J. Jelani, N. Ahmad, and M. I. Akhtar, "Experimental investigation on slope runoff, sediment, and hydraulic parameters under different underlying

surface," *Sinergi*, vol. 29, no. 1, pp. 251-258, 2025, doi: 10.22441/sinergi.2025.1.023
[24] O. Augusto Filho and M. A. Fernandes, "Landslide analysis of unsaturated soil slopes based on rainfall and matric suction data," *Bulletin of Engineering Geology and the Environment*, vol. 78, no. 6, pp. 4167–4185, Sep. 2019, doi: 10.1007/s10064-018-1392-5.
[25] L. Li, Y. Li, and Y. Xu, "Instability evolution of expansive soil slope due to short duration-varying intensities of rainfall," *Engineering Failure Analysis*, vol. 161, no. March, 2024, doi: 10.1016/j.engfailanal.2024.108313.